

M. Fabrizio^{1,2}, M. Nonino³, G. Bono^{2,4}, F. Thèvenin⁵,
M. Monelli⁶, P.B. Stetson⁷, A. Walker⁸ and The Carina Project

¹INAF – OATe, Italy; ²ToV, Italy; ³INAF – OATs, Italy; ⁴INAF-OAR, Italy; ⁵OCA, France; ⁶IAC, Spain; ⁷DAO – HIA, Canada; ⁸NOAO – CTIO, Chile

Abstract. Multi-object spectrographs (MOS) available at the 10m class telescopes disclosed a new scenario concerning the structure and the evolution of nearby dwarf galaxies. They typically display a broad metallicity distribution, suggesting that the environment plays a key role in the chemical evolution of these fluffy stellar systems. Moreover, there is evidence that dwarf galaxies show a complex kinematic structure probably reminiscent either of a disk or of a bulge. We present preliminary results concerning the Carina kinematic structure. We are using a very large data set of homogeneous radial velocity measurements covering the entire body of the galaxy. We found a clear evidence of a rotational pattern in this system. Together with the kinematical discussion, we show the accurate iron abundances for a sizable sample of red giants in the Carina based on spectra collected with UVES at ESO/VLT. The opportunity to collect data with a MOS@E-ELT for a sizable sample of stars with deep magnitudes (22-25) will allow us for the first time to investigate the chemical composition of unevolved (main sequence) and minimally (subgiant) evolved stars in several nearby galaxies. We present simulations concerning selected dSph and dlrr.

Introduction. The Local Group (LG) is a fundamental laboratory to constrain galaxy formation and evolution. Carina dSph stands out among LG galaxies for its Star Formation (SF) activity extended over many Gyr. Deep and accurate photometry disclosed that Carina experienced at least three SF episodes with ages of 2, 3–6 and 11–13 Gyr (Mighell 1990; Smecker-Hane et al. 1996; Hernandez et al. 2000; Rizzi et al. 2003; Monelli et al. 2003; Bono et al. 2010). Moreover, Carina shows a complex kinematic structure, as suggested by Fabrizio et al. (2011), with evidence of sub-structures with transition properties. In this context, Carina is a cornerstone for the future instrumentations available at the E-ELT, and in particular for the multi-object spectrographs. Indeed, we undertook a detailed spectroscopic analysis of Carina stars using low, medium and high resolution spectra to provide homogeneous measurements of iron and alpha-element abundances and to constrain the kinematic properties of the different subpopulations.

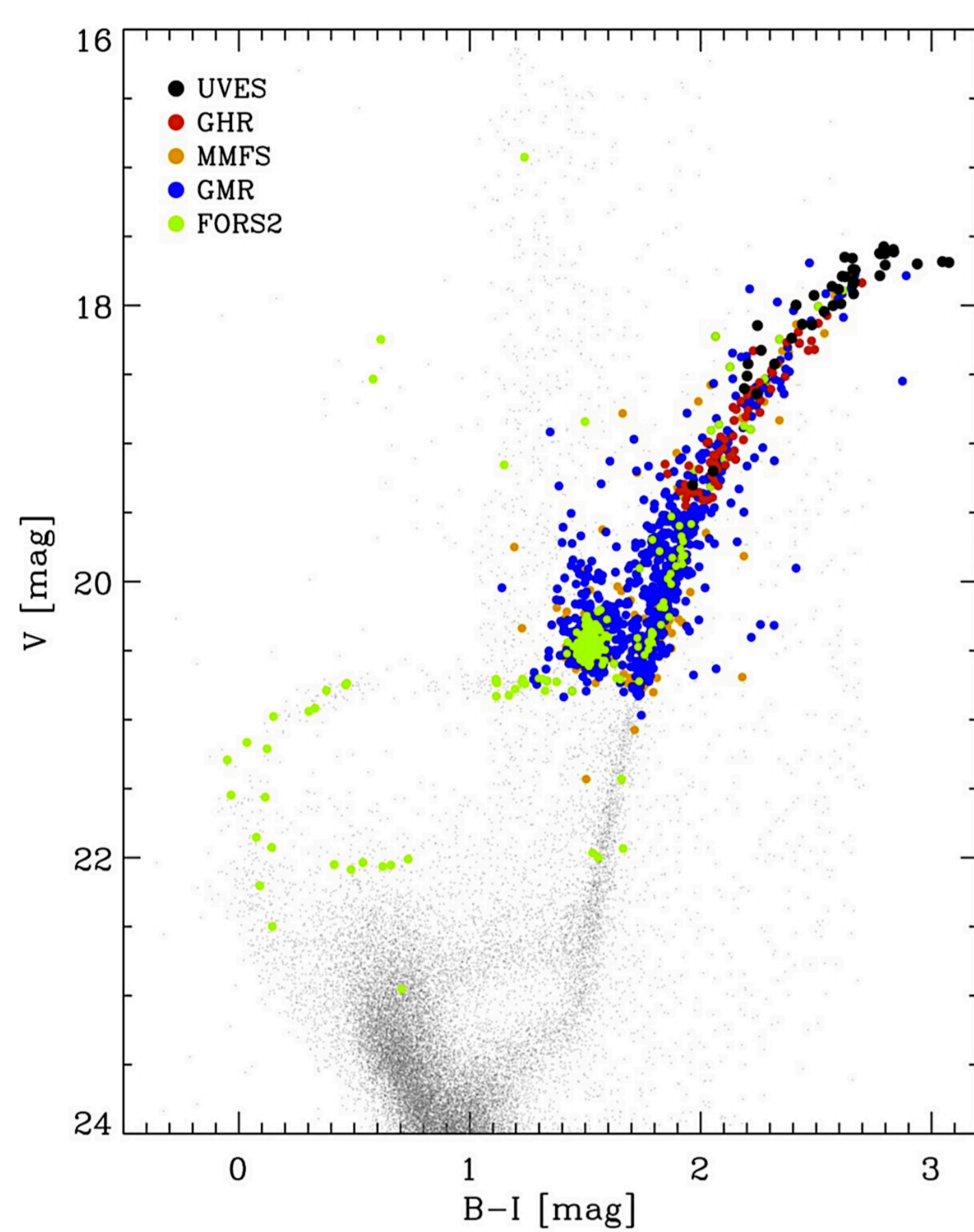


Fig. 1. The use of several multi-object spectrographs available at 10m class telescopes allowed us to assemble a large dataset of spectroscopic targets that covers the entire body of the Carina dwarf spheroidal galaxy. In particular, we used archival and proprietary data for UVES (R~40000), GIRAFFE (HR~20000, LR~6000) and FORS2 (R~2000) at the ESO/VLT, complemented by data from MMFS at the Magellan (R~20000, Walker et al. 2007). We ended up with a total sample of ~2500 stars, with an accurate measure of radial velocity (RV, Fabrizio et al. 2011), identifying ~1370 Carina candidate stars ($180 < RV < 260$ km s⁻¹). In this V vs $B-I$ color-magnitude diagram are plotted, with the labeled color coding, the various spectroscopic targets belonging to Carina.

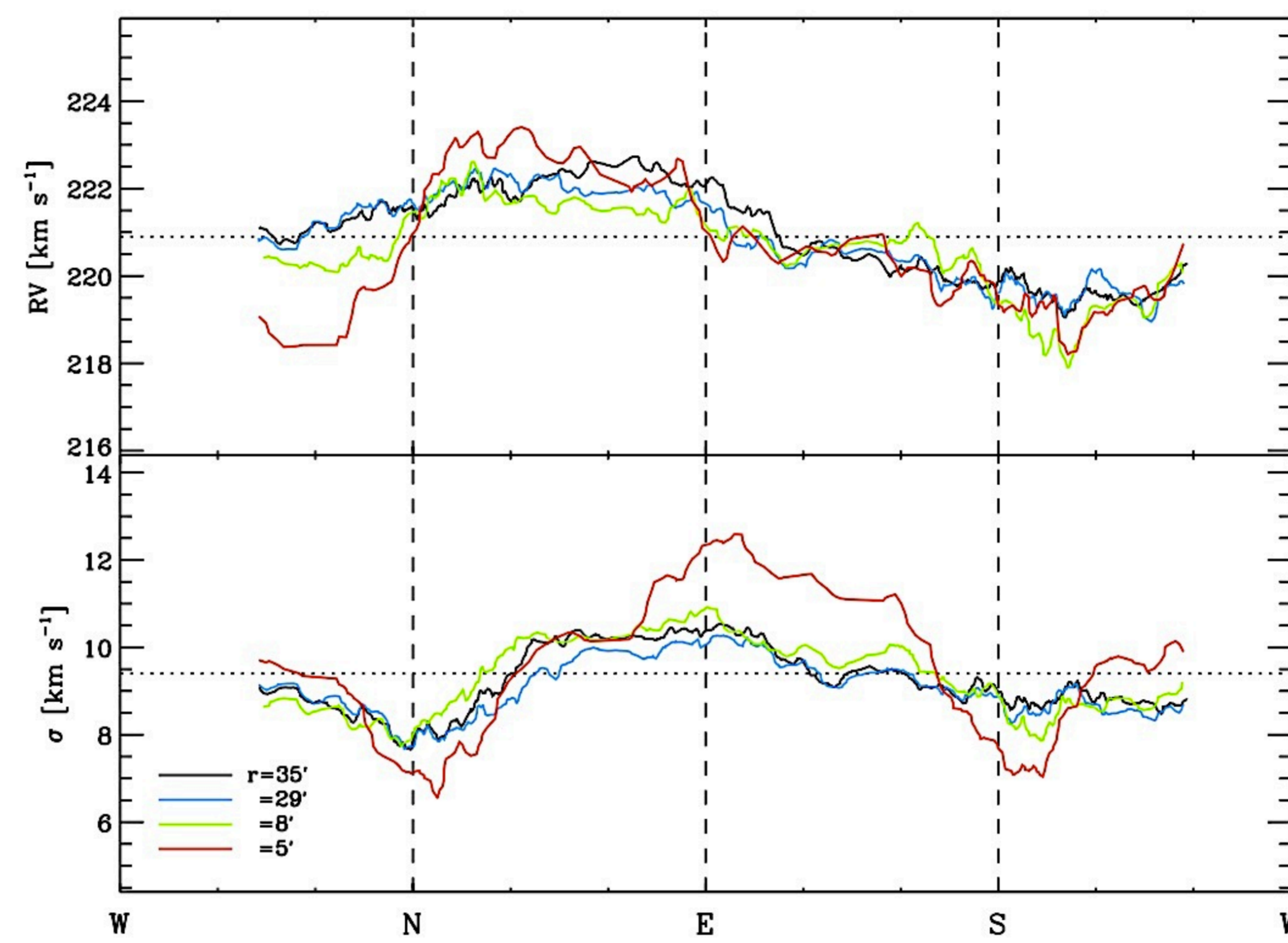


Fig. 2. The entire spectroscopic sample (see fig.1), based over more than 1370 Carina candidate stars, allowed us to analyze the mean RV (top) and the dispersion (bottom) as function of the angle on the sky. Different colored lines are relative to different annuli, from 5' to 35', and are labeled. It is clear that we are facing with a rotational pattern, with an amplitude of ~3 km s⁻¹. More interesting is the fact that exist a transition in the innermost region, inside the core radius (8'). It is noteworthy that the ratio between the rotational velocity and the dispersion is of the order of few tenths, suggesting that Carina is a system gas pressure supported, though it shows a rotation (Fabrizio et al. 2013, in prep.).

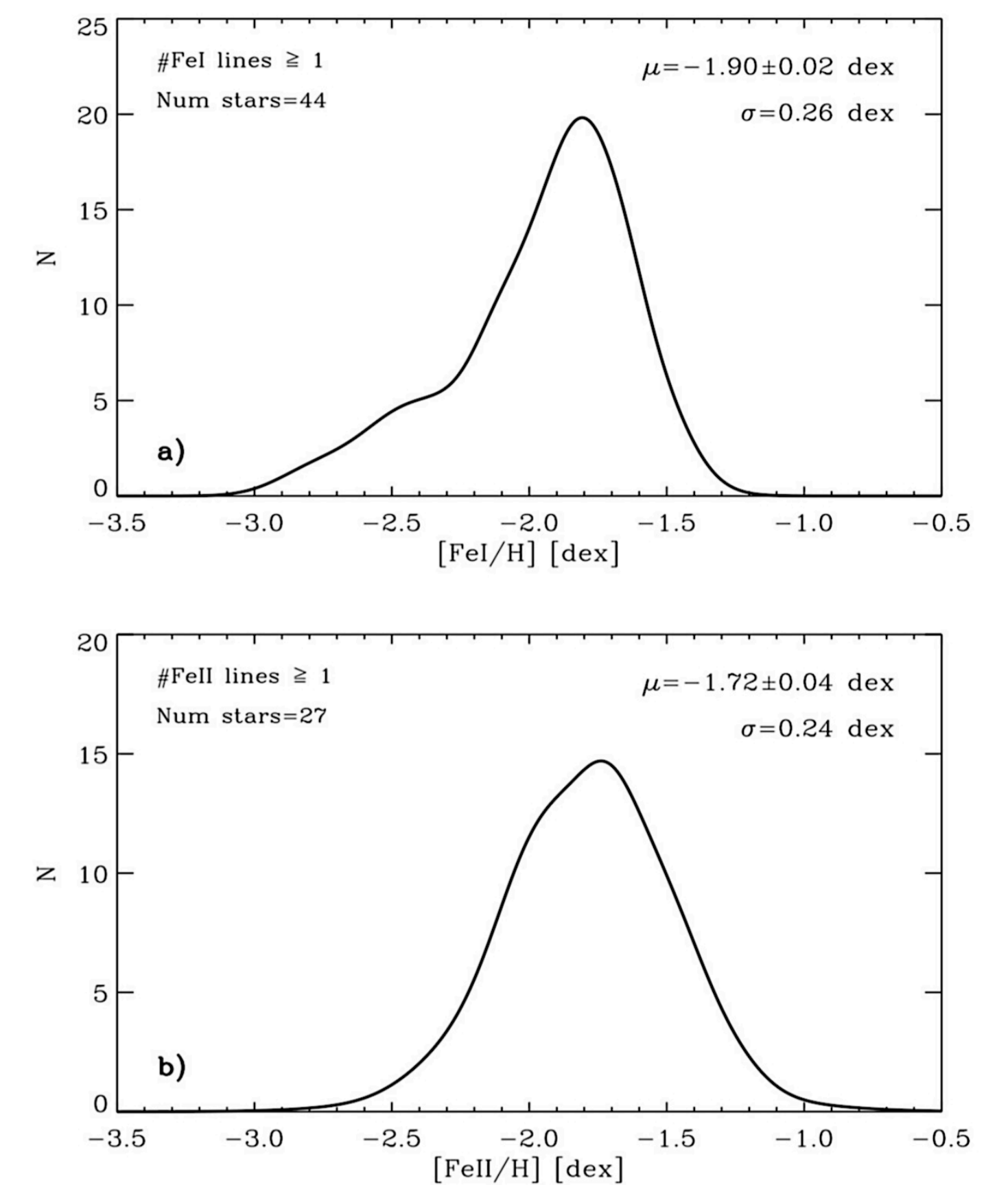


Fig. 3. We used the high-resolution spectra collected with UVES (see fig.1) to obtain accurate iron abundance measurements for 44 red giants in the Carina dSph galaxy. The figure here shows the metallicity distributions of Carina stars based on FeI (top) and FeII (bottom) lines. The weighted means and the weighted standard deviations are labeled, together with the sample size. We found that the range in iron abundances covered by Carina RGs (~1 dex) agrees quite well with similar estimates based on high-resolution spectra (e.g. Lemasle et al. 2012). However, it is a factor of two/three smaller than abundance estimates based on the near IR CaII triplet (Koch et al. 2006). Moreover, for the 27 stars for which we measured both FeI and FeII abundances we found evidence of NLTE effects between neutral and singly-ionized iron abundances (more details in Fabrizio et al. 2012).

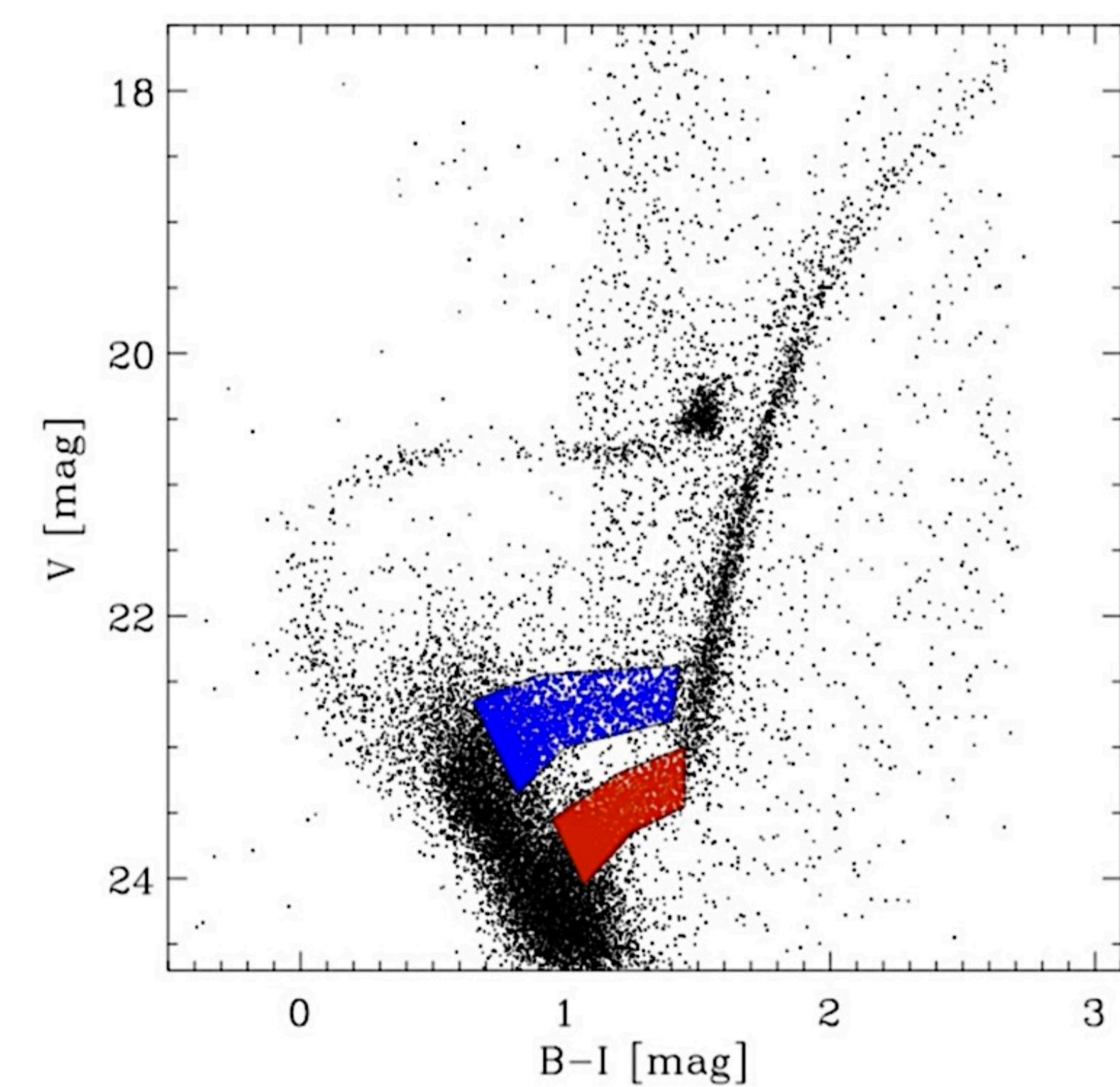


Fig. 4. We push up the capabilities of a MOS mounted at the E-ELT using Carina as a benchmark case. We found that the sub-giant (SG) stars belonging to the two main stellar populations in Carina, ~12 and ~6 Gyr, will be accessible at the limiting magnitude of $V \sim 24$ mag. An instrument with high-multiplexity and a FoV of the order of $10' \times 10'$ could allow us to collect a sizable sample of targets for each pointing over the entire body of the galaxy. In particular, we could observe more than 130+40 SG stars in the outer regions (bottom panel, yellow square) up to 600+400 SGs in the inner one (cyan square). We also performed several feasibility tests with the E-ELT Spectroscopic ETC 2.14. In particular, with the typical observational conditions/limitations (J-band, seeing~0.8", airmass~1.2, total exp. time ~1 hr), we choose three important spectral resolutions ($R=3000, 6000, 20000$) and the Ground-Layer AO (GLAO). We reach a satisfactory signal-to-noise ratio (SNR~30) to obtain RV ($R \sim 3000$) and preliminary abundances ($R \sim 6000$) in a single night, up to the old SG ($V \sim 24$). The GLAO can allow us the detailed abundance measurements ($R \sim 20000$) only up to the intermediate SG ($V \sim 23$).

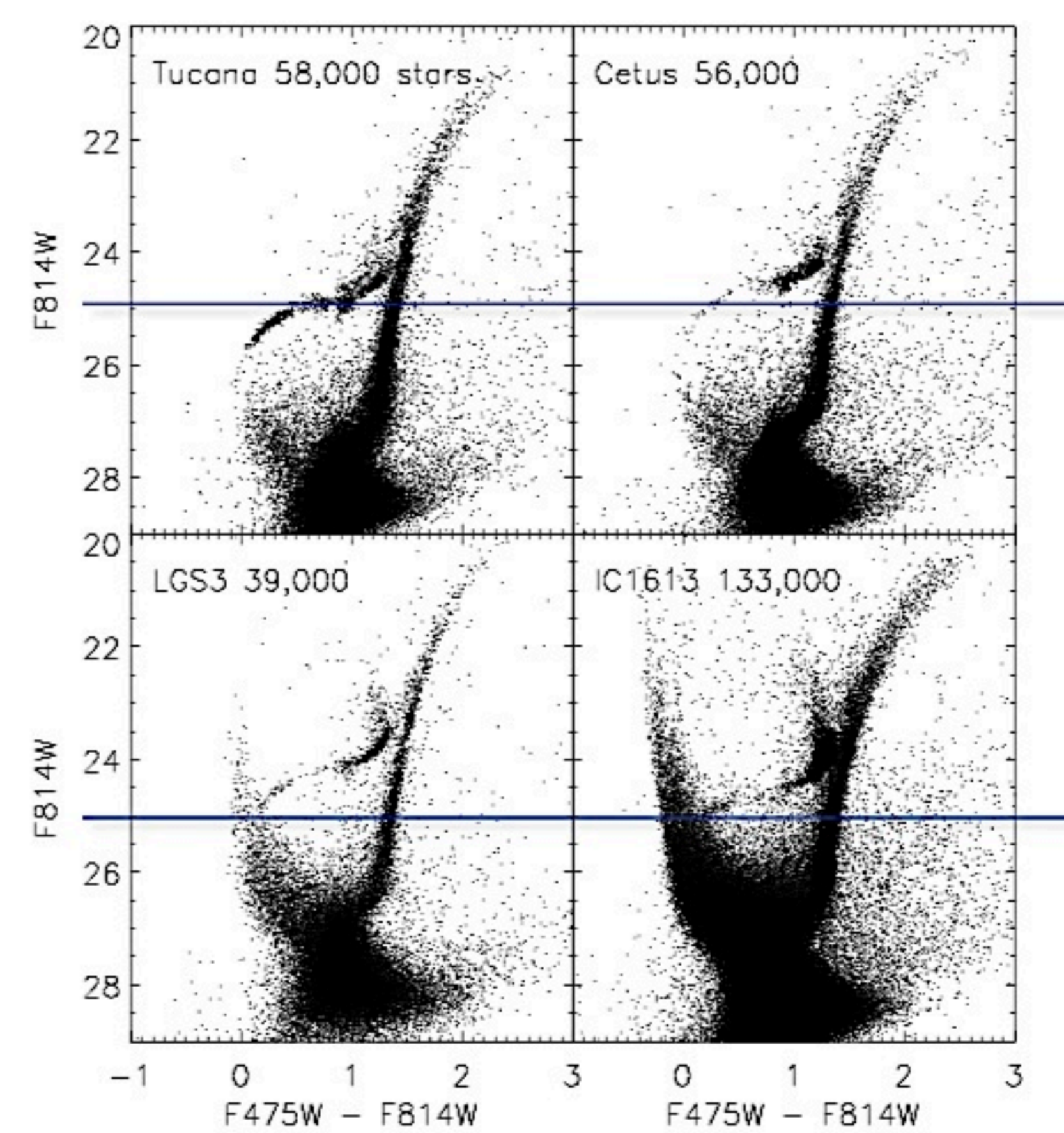
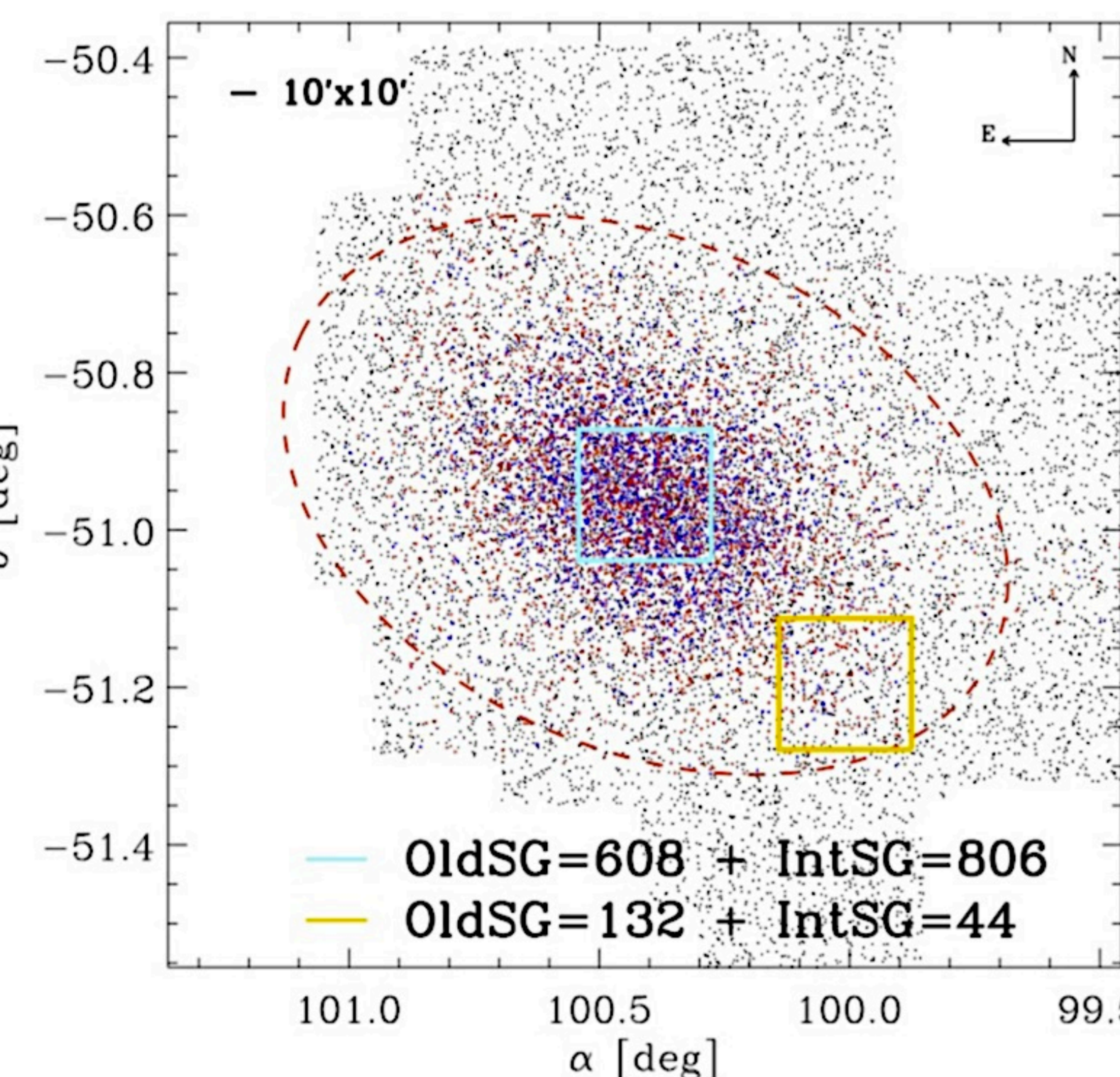


Fig. 5. We could extend the spectroscopic analysis to the other Local Group dwarf galaxies. Here we show the CMDs for two dSphs (Tucana and Cetus, Monelli et al. 2010a,b) and two dwarf Irregulars (LGS3 and IC1613, Hidalgo et al. 2011; Skillemn et al. 2013 in prep.). The blue lines display the limiting magnitude $I=25$ mag. It is clear that not only the RG stars became accessible, in which there are a mixing of populations with different ages, but also the helium burning regions (horizontal branch and red clump) that are the tracers of homologous stellar ages. Moreover, for the dlrrs will be possible to investigate the youngest main sequence stars, allowing the complete coverage of the chemical enrichment histories of these complex and fundamental systems.

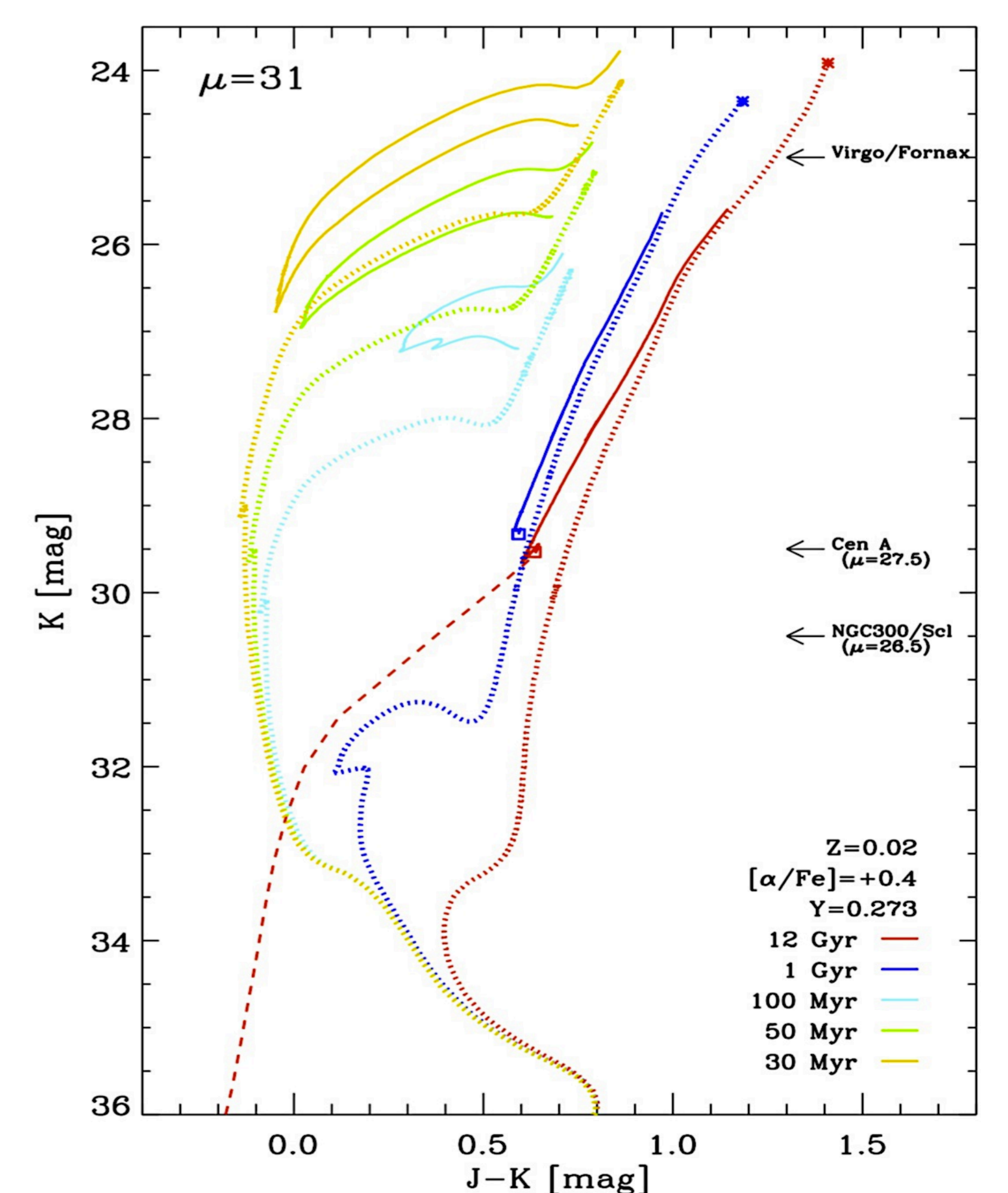


Fig. 6. We also performed a theoretical experiment to understand the limit of MOS@E-ELT, extending our analysis beyond the Local Group. A set of isochrones (from Teramo-BaSTI database, Pietrinfermi et al. 2006), in the K vs $J-K$ CMD, is shown simulating a system with a complex star formation history. We show the oldest population at ~12 Gyr, an intermediate-age population at ~1 Gyr, and a younger population in a range of 30-100 Myr. We applied a distance modulus of the order of Virgo or Fornax clusters, and we found that, by adopting a limiting magnitude of $K \sim 25$ (top arrow), we would have access to the brighter portion of the RGBs. This means that we can obtain important constraints on the kinematics and abundances of these distant systems. Furthermore, we indicate the same limiting magnitude reachable for other two systems (CenA, NGC300 or Sculptor group). In this case, the capabilities of E-ELT will allow us to obtain spectroscopic measurements for the entire extension of RGB and young MS, while, for the closer one, we also have the opportunity to investigate the HB stars.

Conclusions

Top level requirements for MOS@E-ELT

Large FoV	>7'x7' (10'x10')
Target density	10s arcmin ⁻²
Spatial resolution	GLAO
Spectral resolution	> 3000 – 200000
Wavelength coverage	1.0 – 2.2 μm
Limiting magnitude	J, H, K < 25 mag
S/N	~ 30 (kin) – 60 (abund)

Simultaneous multiplexity between low/medium and high resolution fibers

References

Bono, G. et al. 2010, PASP, 122, L111
Fabrizio, M. et al. 2011, PASP, 123, 384
Fabrizio, M. et al. 2012, PASP, 124, 519
Hidalgo, S.L. et al. 2011, ApJ, 730, 14
Hernandez, X. et al. 2000, MNRAS, 317, 831
Koch, A. et al. 2006, AJ, 131, 895
Lemasle, B. et al. 2012, A&A, 538, 100
Mighell, K. J. 1990, A&AS, 82, 1

Monelli, M. et al. 2003, AJ, 126, 218
Monelli, M. et al. 2010a, 720, 1225
Monelli, M. et al. 2010b, 722, 1864
Pietrinfermi, A. et al. 2006, 642, 797
Rizzi, L. et al. 2003, ApJL, 589, L85
Smecker-Hane, T. A. et al. 1994, AJ, 108, 507
Walker, M. G. et al. 2007, ApJS, 171, 389

Contact: michele.fabrizio@roma2.infn.it